

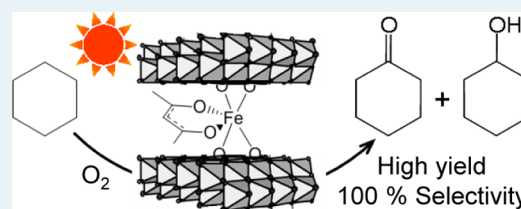
Efficient and Selective Photocatalytic Cyclohexane Oxidation on a Layered Titanate Modified with Iron Oxide under Sunlight and CO₂ Atmosphere

Hideya Hattori, Yusuke Ide,* Shuhei Ogo, Kei Inumaru, Masahiro Sadakane, and Tsuneji Sano

Department of Applied Chemistry, Graduate School of Engineering, Hiroshima University, 1-4-1 Kagamiyama, Higashi-Hiroshima 739-8537, Japan

ABSTRACT: Layered titanates modified with molecular level iron oxide were synthesized by a reaction between $K_{0.7}Ti_{1.73}Li_{0.27}O_4$ and Fe(III) acetylacetonate complex using the dodecylammonium-exchanged layered titanate as intermediate. The iron oxide-modified layered titanates were used as catalysts for selective oxidation of cyclohexane with molecular oxygen under sunlight irradiation. The catalysts produced cyclohexanone and cyclohexanol with high selectivity up to 100% and showed cyclohexane conversion comparable to that obtained over a commercially available TiO_2 (P25), depending on the amount of the attached iron oxide. The results were explained by the molecular cognitive cyclohexane adsorption ability of the catalysts, that is, the inhibition of the successive oxidation of the formed products. The cyclohexane conversion over the iron oxide-modified layered titanates was substantially improved with 100% selectivity maintained by conducting the reaction under a CO_2 atmosphere.

KEYWORDS: layered titanate, iron oxide, photocatalysis, cyclohexane, sunlight



INTRODUCTION

Production of chemicals and fuels through heterogeneous photocatalysis driven by sunlight is one of the most compelling objectives in modern chemistry. Titanium dioxide is a promising material for the purpose due to availability, low toxicity, and chemical stability; however, it responds only to UV light, occupying 3–4% of sunlight, and tends to be nonselective for synthetic reactions.¹ Accordingly, after the discovery on the photocatalysis of TiO_2 ,^{2,3} a great deal of endeavor has been spent on modifying TiO_2 by heteroelemental doping^{4,5} and hybridization with organic dyes⁶ and nanoparticles⁷ as well as designing novel catalysts, such as molecular-sieve-like TiO_2 ^{8–11} and non- TiO_2 materials,^{12–17} for efficient and selective photocatalysis under sunlight. In particular, iron doping and iron or iron oxide modification of TiO_2 has merit in that iron is also harmless and abundant in nature; however, only a limited number of works have been reported to attain increased UV light-induced activity and visible light response of TiO_2 ,^{18–20} which are necessary for the application under sunlight. Moreover, there are few reports on photocatalytic synthetic reactions over such materials under sunlight.²¹ In this article, we report the successful synthesis of new photocatalyst composed of titania nanosheets and molecular-level iron oxides, which exhibits a high level of activity for a photocatalytic organic synthesis under sunlight. A layered titanate was chosen to be modified with molecular-level iron oxide, since the iron species is immobilized in the interlayer space of a layered titanate to possibly give “pillared” clay-type material with molecular concentration and recognition abilities,^{9,10,22} which are useful for organic syntheses.

Selective cyclohexane oxidation is one of the most important synthetic reactions in chemical industry, since the partially oxidized products, cyclohexanone and cyclohexanol, are an intermediate in ϵ -caprolactam synthesis, which is used in the manufacture of nylon polymers. Increasing environmental concerns call for the development of green processes for the reaction alternative to the existing processes. Recently, photocatalytic cyclohexane oxidations in heterogeneous systems under visible light irradiation have been actively investigated.^{23–27} In this study, we report a high level of the photocatalytic activity of the presently developed material for selective cyclohexane oxidation under sunlight. The result shows a potential application of the present material to the commercial production of cyclohexanone and cyclohexanol in an environmentally and economically benign fashion.

EXPERIMENTAL SECTION

Photocatalyst Synthesis. A layered titanate, $K_{0.7}Ti_{1.73}Li_{0.27}O_4$ (named KTLO),^{28,29} was reacted with an aqueous solution of dodecylamine hydrochloride (>97%, Tokyo Chemical Industry Co., Ltd.) according to the reported procedure²⁹ to prepare the dodecylammonium-exchanged layered titanate (named $C_{12}N^+$ -TLO). $C_{12}N^+$ -TLO (0.6 g (2.9×10^{-3} mol)) was added to a solution of Fe(III) acetylacetonate complex (named $Fe(acac)_3$, Wako Pure Chemical Industries, Ltd.) in a mixed solvent (200 mL,

Received: May 30, 2012

Revised: July 20, 2012

Published: July 26, 2012

ethanol/hexane = 3:17 v/v), and the mixture was stirred at room temperature for 3 days. The product was separated by centrifugation (3500 rpm, 20 min), washed repeatedly with the same solvent, and then washed with a mixed solution of ethanol and 0.1 mol L⁻¹ of aqueous hydrogen chloride (1:1 v/v). The amount of the added Fe(acac)₃ was tuned (1.5 × 10⁻³ or 2.9 × 10⁻³ mol) to control the amount of the attached Fe(acac)₃ on the titanate. The iron oxide-modified layered titanate thus obtained was named FeO_x-TLO, where *x* denoted the number of the attached Fe (groups) per a unit cell of K_{0.7}Ti_{1.73}Li_{0.27}O₄. The layered titanate in which only the particle outer surface was modified with iron oxide (named FeO@KTLO) and a commercially available TiO₂ (Aerosil P25) modified with iron oxide (named FeO@P25) were synthesized in a way similar to that in the synthesis of FeO_x-TLO, except that pristine KTLO and P25 were used, respectively, and the products after Fe(acac)₃ adsorption were washed with the ethanol/hexane mixed solvent and then calcined at 500 °C for 1 h.

Materials Characterization. X-ray diffraction (XRD) patterns of solid products were collected using a powder X-ray diffractometer (Bruker D8 Advance) with graphite-monochromatized Cu Kα radiation at 40 kV and 30 mA. UV-vis spectra were recorded with a Jasco V-579 UV/vis/NIR spectrophotometer. X-ray photoelectron spectra (XPS) were taken with a Kratos ESCA-3400 electron spectrometer, where the binding energies were calibrated by the O 1s peak. Thermogravimetric-differential thermal analysis (TG-DTA) curves were collected using a SSC/5200 apparatus (Seiko Instruments). The sample was heated from room temperature to 800 °C in an air flow (50 mL min⁻¹) at a rate of 10 °C min⁻¹. The crystal morphology of products was observed by scanning electron microscopy (SEM, Hitachi S-4800), and the elemental mapping was conducted by SEM and energy-dispersive X-ray analysis. Inductively coupled plasma optical emission spectroscopy was performed on a Seiko SPS7000. The solid products were decomposed for the measurements with an aqueous H₂SO₄ solution. Nitrogen adsorption isotherms at -196 °C were obtained using a conventional volumetric apparatus (BELSORP-mini, Bel Japan). Prior to the adsorption measurements, the samples were evacuated at 120 °C for 12 h.

Photocatalytic Tests. A mixture of catalyst (30 mg) and O₂-saturated acetonitrile (18 mL) solution of cyclohexane (2 mL) in a stainless-made closed container equipped with Pyrex glass (75 mL) was irradiated with solar simulator (San-Ei Electric Co., Ltd.) at 42 °C, under shaking. The container was placed ~30 cm away from the light source to irradiate 1 solar (1000 W m⁻²)-power light to the mixture. After the reaction, the gas-phase product was analyzed by GC-TCD (Shimadzu GC-8A). The solution was mixed with toluene (as internal standard) and then recovered by filtration, and the resulting supernatant was analyzed by GC-FID (Shimadzu GC-2014). Only three products, cyclohexanone, cyclohexanol, and CO₂, were detected in the present study. The intermediates, such as cyclohexyl hydroperoxide, were not detected.

Adsorption Tests. Adsorption was done in a way similar to that conducted in the photocatalytic conversions except that 10 mg (~30 μmol) of the catalyst and a mixed solution (20 mL) of cyclohexane and cyclohexanone (~90 μmol for each compound) in acetonitrile, which was not bubbled with O₂, were shaken in the dark at room temperature for 6 h.

Apparent Quantum Yield Measurement. The full arc from a 500 W Xe lamp (Ushio) was monochromated using SM-25 (Bunkoukeiki) and then used to irradiate a mixture of

catalyst (30 mg) and O₂-saturated acetonitrile (18 mL) solution of cyclohexane (2 mL) in the container. The light intensity of the monochromated Xe lamp was determined using a spectroradiometer, USR-45D (Ushio).

RESULTS AND DISCUSSION

Photocatalyst Synthesis. The interlayer modification of KTLO with molecular-level iron oxide was performed by adsorption with Fe(acac)₃. A direct reaction between KTLO and Fe(acac)₃ did not lead the intercalation of the complex into the interlayer space; therefore, the interlayer K⁺ was first exchanged with dodecylammonium cation to expand the interlayer space, and the resulting C₁₂N⁺-TLO was reacted with Fe(acac)₃, followed by removal of the dodecylammonium with washing. Similar procedures have often been employed to introduce bulky silane coupling reagents into the interlayer space of layered silicates and titanates.^{30,31}

The XRD patterns of KTLO, C₁₂N⁺-TLO, and FeO_{0.13}-TLO before and after the washing are depicted in Figure 1. The basal

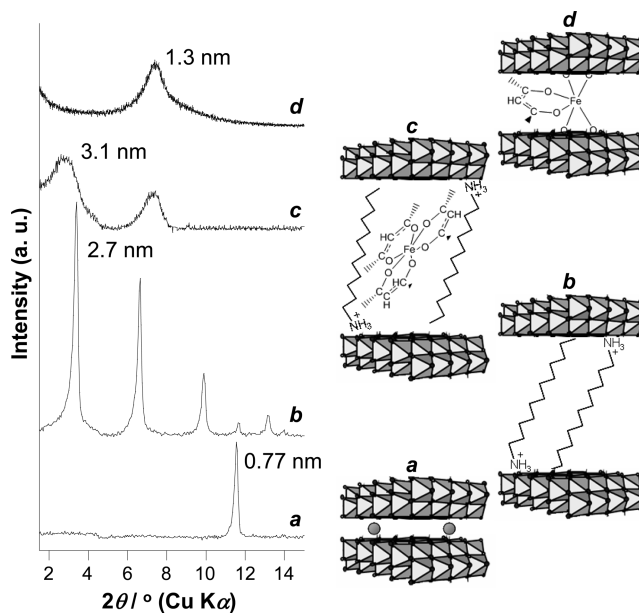


Figure 1. XRD patterns of (a) KTLO, (b) C₁₂N⁺-TLO and FeO_{0.13}-TLO before (c) and after (d) washing. Insets show the schematic structures of the corresponding products.

spacing (2.7 nm) of C₁₂N⁺-TLO increased to 3.1 nm and then decreased to 1.3 nm after the reaction with Fe(acac)₃ and the subsequent washing, respectively. The elemental mapping of FeO_{0.13}-TLO revealed that Fe was not concentrated on the particle outer surface but distributed entirely within the particle (Figure 2). The XPS spectrum of the FeO_{0.13}-TLO confirmed the presence of Fe³⁺ on the surface^{19,20} (data not shown). Since Fe(acac)₃ has been reported to irreversibly react with the surface Ti—OH group to form a Ti—O—Fe covalent bond via a ligand exchange reaction,¹⁹ the data provided above indicate that Fe(acac)₃ is immobilized on the interlayer space of KTLO, and dodecylammonium is removed. In the XRD pattern of the FeO_{0.13}-TLO, the peak attributed to the (200) lattice plane of the KTLO was observed at 49°, confirming that the structural regularity on the layered titanate is retained after the modification with Fe(acac)₃.

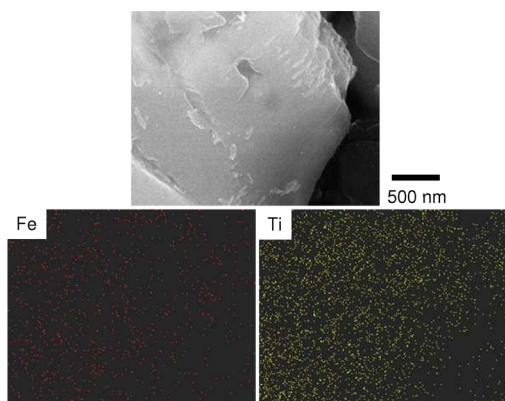


Figure 2. SEM image of $\text{FeO}_{0.13}$ -TLO and the corresponding elemental mapping.

The composition of the attached iron oxide species in $\text{FeO}_{0.13}$ -TLO was estimated to be $\text{Fe}(\text{C}_5\text{H}_7\text{O}_2)_{0.8}$, which was on the basis of the amounts of Fe and acetylacetonate ligand determined by the ICP of the dissolved product (Table 1) and

Table 1. Character of FeO_x -TLO

	Fe/wt %	attached Fe^a	gallery height/ nm^b	Fe-Fe distance/ nm^c
$\text{FeO}_{0.09}$ -TLO	2.7	$\text{Fe}(\text{C}_5\text{H}_7\text{O}_2)_{1.8}$	0.6	1.1
$\text{FeO}_{0.13}$ -TLO	4.0	$\text{Fe}(\text{C}_5\text{H}_7\text{O}_2)_{0.8}$	0.8	0.9

^aOn the assumption that all mass loss from 300 to 500 °C in the TG curves of FeO_x -TLO (Figure 3) is due to the oxidative decomposition of acetylacetonate ligands. ^bThe single layer thickness of KTLO (0.5 nm)³² was subtracted from the observed basal spacing. ^cCalculated as $(2ab/x)^{1/2}$, ab and x denote basal area of KTLO ($0.38 \times 0.30 \text{ nm}^2$) and Fe/TLO molar ratio, respectively.³³

the TG-DTA curves of the product (Figure 3), respectively. The amount of the attached $\text{Fe}(\text{C}_5\text{H}_7\text{O}_2)_{0.8}$ was 0.13 groups per $\text{Ti}_{1.73}\text{Li}_{0.27}\text{O}_4$ unit cell, which was equivalent to the distance between the adjacent iron oxides of 0.9 nm (Table 1). When the amount of the added $\text{Fe}(\text{acac})_3$ was smaller, the iron oxide-modified layered titanate with smaller basal spacing (1.1 nm), a

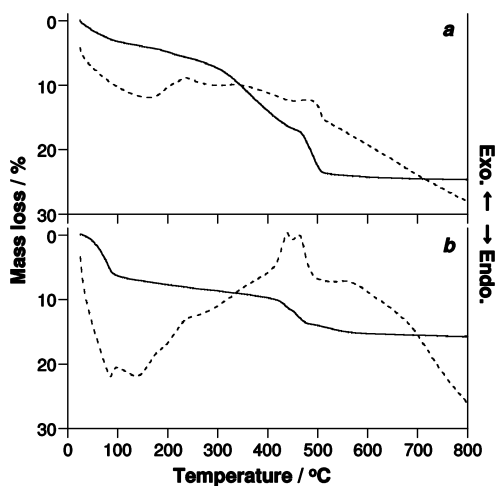


Figure 3. TG (solid)–DTA (dashed) curves of (a) $\text{FeO}_{0.09}$ -TLO, and (b) $\text{FeO}_{0.13}$ -TLO recorded in air.

different kind of the attached iron oxide species ($\text{Fe}(\text{C}_5\text{H}_7\text{O}_2)_{1.8}$), and a smaller amount of the attached $\text{Fe}(\text{acac})_3$ (0.09 groups per a $\text{Ti}_{1.73}\text{Li}_{0.27}\text{O}_4$ unit cell) was synthesized. The results are summarized in Table 1.

Figure 4 shows the N_2 adsorption isotherms of FeO_x -TLO and pristine KTLO. The N_2 adsorption capacity of KTLO was

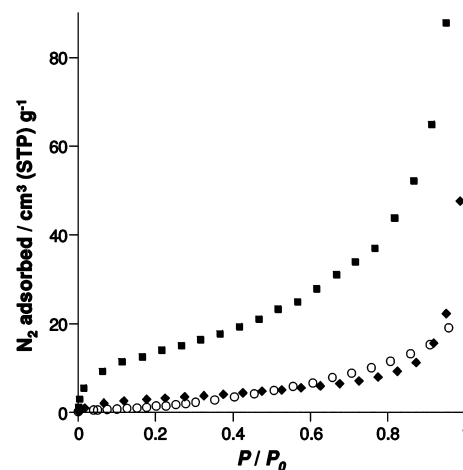


Figure 4. N_2 adsorption isotherms of (O) KTLO, (◆) $\text{FeO}_{0.09}$ -TLO, and (■) $\text{FeO}_{0.13}$ -TLO.

enhanced after the modification with iron oxide. The N_2 adsorption capacity of $\text{FeO}_{0.13}$ -TLO was larger than that of $\text{FeO}_{0.09}$ -TLO. Smaller gallery height and a larger amount of the remaining acetylacetonate ligand of $\text{FeO}_{0.09}$ -TLO possibly made the access of N_2 into the interlayer space more difficult (Table 1). Judging from the distance between the adjacent iron oxides and the gallery height, $\text{FeO}_{0.09}$ -TLO and $\text{FeO}_{0.13}$ -TLO have the interlayer pores to concentrate cyclohexane ($0.5 \times 0.5 \times 0.4 \text{ nm}^3$). The composition of iron oxide species ($\text{Fe}(\text{C}_5\text{H}_7\text{O}_2)_{0.8}$, that is, only one-third of the acetylacetonate ligands remain) of $\text{FeO}_{0.13}$ -TLO suggests that $\text{Fe}(\text{acac})_3$ is immobilized on the titanate sheets to pillar the adjacent sheets, as schematically shown in the inset of Figure 1d. The attachment by bridging three or four Ti–OH's on the titanate sheet seems impossible taking the flat surface of the titanate sheet and the spherical geometry of free $\text{Fe}(\text{acac})_3$ into account. On the other hand, $\text{Fe}(\text{acac})_3$ is possibly immobilized on the titanate sheet in a dipodal fashion to leave two acetylacetonate ligands in $\text{FeO}_{0.09}$ -TLO.

The UV–vis diffused reflectance spectra of FeO_x -TLO are depicted in Figure 5, together with that of KTLO and $\text{FeO}@$ KTLO. FeO_x -TLO showed shoulders around 420 nm and absorption bands centered at 490 nm. In the absorption spectrum of $\text{Fe}(\text{acac})_3$, an absorption band due to d–d transition in the acetylacetonate ligands was observed at 430 nm (Figure 5e). Therefore, the former absorption bands for FeO_x -TLO are assignable to the d–d transition in the attached acetylacetonate ligands. On the other hand, it is difficult to assign the latter absorption bands for FeO_x -TLO. $\text{Fe}(\text{III})$ -grafted TiO_2 , prepared by the impregnation with FeCl_3 , showed a weak absorption band centered around 500 nm ascribable to electron transfer from the valence band of TiO_2 to Fe^{3+} .²⁰ Similar absorption bands were observed for $\text{Fe}(\text{acac})_3$ -modified TiO_2 (P25) after calcination,¹⁹ $\text{FeO}@$ P25,²¹ and $\text{FeO}@$ KTLO (Figure 5d). Therefore, the absorption around 490 nm for FeO_x -TLO implies the presence of molecular level iron oxides.

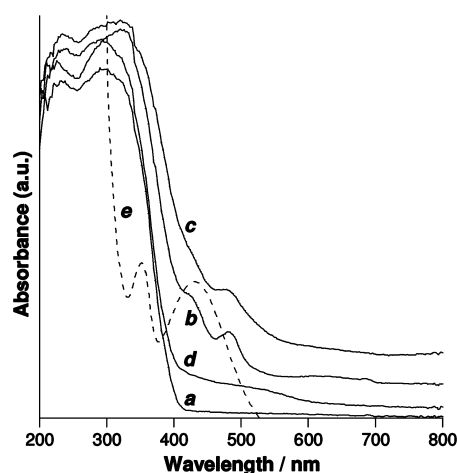


Figure 5. Diffused reflectance UV-vis spectra of (a) KTLO, (b) FeO_{0.09}-TLO, (c) FeO_{0.13}-TLO, and (d) FeO@KTLO. Dashed line (e) denotes UV-vis absorption spectrum of Fe(acac)₃ in an ethanol/hexane mixture.

Photocatalytic Activity. To assess a high level of photocatalytic activity of FeO_x-TLO toward selective cyclohexane oxidation under sunlight, the activity of FeO_x-TLO was compared with those of a commercially available TiO₂ (P25), FeO@P25²¹ and FeO@KTLO under the same irradiation conditions and with the same amount of photocatalysts (Table 2). FeO_x-TLO showed selectivity up to 100% (Table 2, entries 1, 2, 5, 8), which was considerably higher than that obtained on P25 (Table 2, entry 9). The extremely high selectivity resulted from the suppression of CO₂ evolution. FeO_{0.13}-TLO gave the best result, with the conversion comparable to that obtained on P25 (Table 2, entries 5, 8, and 9).

To the best of our knowledge, the activity obtained on FeO_{0.13}-TLO at 6 h of sunlight irradiation (0.14% conversion, ~100% selectivity, and 28% apparent quantum yield at 380 nm) was superior or comparable to those that had been reported for photocatalytic cyclohexanone and cyclohexanol production under visible light,^{23–27} although the present material is cheap and abundant. For example, 0.09% conversion and >99% selectivity were obtained on Cr/Ti/Si ternary mixed oxide.²⁷ The activity of FeO@P25²¹ was lower than that of

FeO_x-TLO under identical conditions (Table 2, entries 2, 5, 8, 10, and 11), showing a merit of the presently proposed material design. Further improvement of the photocatalytic activity of FeO_x-TLO seems possible by controlling reaction environments, since we have reported the positive effects of a reaction environment, such as the presence of a target product in the starting mixture¹⁰ and CO₂ atmosphere,^{21,34} on photocatalytic selective oxidations. Indeed, cyclohexane conversion of FeO_x-TLO was substantially improved, with 100% selectivity maintained by conducting the reaction under a CO₂ atmosphere (Table 2, entries 1, 4, 5, and 7). The XRD patterns and the UV-vis spectra of FeO_x-TLO did not change after the photocatalytic reaction, and Fe was not detected by the UV-vis absorption spectra of the supernatant after the reaction. Therefore, FeO_x-TLO was stable during the present photocatalysis. As a result, it could be reused without loss of the original activity (Table 2, entries 5 and 6), which was a merit for the practical application.

The roles of the immobilized iron oxide species of FeO_x-TLO in the present photocatalytic cyclohexane oxidation were discussed. When FeO_x-TLO was mixed with a mixture of cyclohexane and cyclohexanone in the dark, cyclohexane was selectively adsorbed (Table 3). The surface Ti-OH (which can

Table 3. Separation of Cyclohexane (CH) and Cyclohexanone (CHone) on FeO_x-TLO.^a

catalyst	amount adsorbed/ μmol		CH/CHone separation
	CH	CHone	
FeO _{0.09} -TLO	43.7	30.0	1.5
FeO _{0.13} -TLO	47.1	25.9	1.8

^aThe catalyst (~30 μmol) was mixed with a mixed solution of CH and CHone (~90 μmol for each compound) in the dark.

interact with cyclohexanone and cyclohexanol) on FeO_x-TLO is occupied with iron oxide species so effectively that interactions between the catalysts and the partially oxidized products are relatively weak. Accordingly, the photocatalytically formed cyclohexanone and cyclohexanol promptly desorb from the active center (interlayer spaces) of FeO_x-TLO, giving the effective and selective formation of the products. As shown in Table 2 (entry 12), only trace amounts of cyclohexanone and

Table 2. Oxidation of Cyclohexane (CH) to Cyclohexanone (CHone) and Cyclohexanol (CHnol) under Simulated Solar Light

entry	catalyst	irradiation time/h	yield/ μmol			selectivity [CHone + CHnol]/% ^b	CH conversion/% ^c
			CHone	CHnol	CO ₂ ^a		
1	FeO _{0.09} -TLO	6	0.90	0.29	trace	>99	0.006
2	FeO _{0.09} -TLO	12	6.4	5.0	trace	>99	0.062
3	FeO _{0.09} -TLO ^d	6	n.d.	trace	trace		
4	FeO _{0.09} -TLO ^e	6	2.7	1.2	trace	>99	0.020
5	FeO _{0.13} -TLO	6	15.4	10.5	n.d.	>99.9	0.14
6	FeO _{0.13} -TLO ^f	6	15.3	10.2	n.d.	>99.9	0.14
7	FeO _{0.13} -TLO ^g	6	18.8	21.2	trace	>99	0.22
8	FeO _{0.13} -TLO	12	22.5	16.2	57.9	>80.0	0.26
9	P25	12	34.0	3.2	144.5	55.5	0.33
10	FeO@P25	6	3.6	trace	trace	>99	0.020
11	FeO@P25	12	4.6	trace	19.6	58.2	0.043
12	FeO@KTLO	6	n.d.	n.d.	67.3		

^aMeasurement error of within 1%. ^b $\{[\text{formed CHone}] + [\text{formed CHnol}]\} / \{[\text{formed CHone}] + [\text{formed CHnol}] + 1/6[\text{formed CO}_2]\} \times 100$. ^c $\{[\text{formed CHone}] + [\text{formed CHnol}] + 1/6[\text{formed CO}_2]\} / [\text{added CH}] \times 100$. ^dSunlight with a wavelength shorter than 420 nm was the cutoff. ^eUnder CO₂ atmosphere (40 kPa). ^fReused after washing with acetonitrile. ^gUnder CO₂ atmosphere (20 kPa).

cyclohexanol formed on FeO@KTLO that did not adsorb cyclohexane and cyclohexanone effectively. This result supports the above idea. FeO_{0.13}-TLO adsorbs cyclohexane more effectively than FeO_{0.09}-TLO due to the larger surface area (Table 1 and 3), giving higher cyclohexane conversion (Table 2). Studies on the catalytic or photocatalytic conversion of organic substrates using zeolites³⁵ and mesoporous materials^{8,10,36} have demonstrated that the separation of target products from the catalysts plays an important role in the efficient formation of the products. Further studies on the nanostructural design of FeO_x-TLO by changing the amount of the attached Fe(acac)₃ and coimmobilizing other functional units^{33,37} are worth conducting to optimize the molecular recognition ability and then the photocatalytic performance.

Another possible role of the immobilized iron oxide is to improve the charge separation efficiency of FeO_x-TLO. When sunlight only with wavelength longer than 420 nm was used to irradiate FeO_{0.09}-TLO, cyclohexanone, cyclohexanol and CO₂ hardly formed (Table 2, entry 3). Therefore, the attached Fe(acac)₃ did not work as a visible light harvester. It should be noted here that the presently designed FeO_x-TLO effectively photocatalyzes cyclohexane using only the UV spectrum of sunlight. It has been suggested that in TiO₂ modified with molecular level iron oxide, the iron oxide accepts electrons generated by the band gap excitation of TiO₂ to improve the charge separation efficiency.^{19,21}

Figure 6 shows the time-dependent change in the yields of cyclohexanone, cyclohexanol, and CO₂ during the photo-

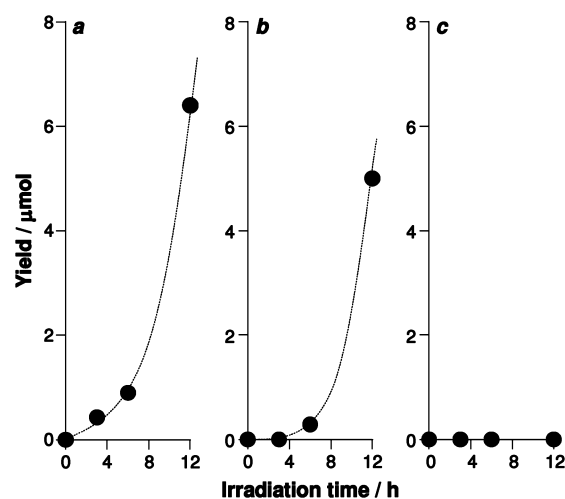


Figure 6. Time-dependent changes in the amounts of (a) cyclohexanone, (b) cyclohexanol, and (c) CO₂ during photooxidation of cyclohexane on FeO_{0.09}-TLO.

catalytic cyclohexane oxidation over FeO_{0.09}-TLO. Almost equivalent amounts of cyclohexane and cyclohexanone formed, and a much smaller amount of CO₂ evolved. From all the results obtained, a possible mechanism for the present reaction was proposed as follows: First, the intercalated cyclohexane is reacted with either a hole or OH[•] (or OH₂^{•+}), which are photogenerated on the titanate valence band of FeO_x-TLO, to form cyclohexyl radical. The formed radical is then reacted with OH[•] (or OH₂^{•+}) and O₂^{•-}, which is derived from the reduction of O₂ by the excited electron on the titanate conduction band, to generate cyclohexanol and cyclohexanone, respectively.^{15,38} The generated products are promptly desorbed from the interlayer space to prevent successive oxidation.

CONCLUSION

In summary, a layered titanate containing immobilized molecular level iron oxide in the interlayer space was successfully synthesized by the reaction between a layered titanate and iron(III) acetylacetonate complex. The obtained material was found to effectively and selectively catalyze the oxidation of cyclohexane to cyclohexanone and cyclohexanol with molecular O₂ under sunlight irradiation. The photocatalytic activity was substantially modified by conducting the reaction under a CO₂ atmosphere. Because of the potential for further nanostructure design of the hybrid photocatalyst, the present result opens up new opportunities for the production of various commodity chemicals in an economically and environmentally favorable fashion.

AUTHOR INFORMATION

Corresponding Author

*E-mail: yusuke-ide@hiroshima-u.ac.jp.

Notes

The authors declare no competing financial interest.

REFERENCES

- Ohtani, B.; Tsuru, S.; Nishimoto, S.; Kagiya, T.; Izawa, K. *J. Org. Chem.* **1990**, *55*, 5551–5553.
- Fujishima, A.; Honda, K. *Nature* **1972**, *238*, 37–38.
- Fujihira, M.; Satoh, Y.; Osa, T. *Nature* **1981**, *293*, 206–208.
- Anpo, M.; Takeuchi, M. *J. Catal.* **2003**, *216*, 505–516.
- Asahi, R.; Morikawa, T.; Ohwaki, T.; Aoki, K.; Taga, Y. *Science* **2001**, *293*, 269–271.
- Youngblood, W. J.; Lee, S.-H. A.; Maeda, K.; Mallouk, T. E. *Acc. Chem. Res.* **2009**, *42*, 1966–1973.
- Primo, A.; Corma, A.; Garcia, H. *Phys. Chem. Chem. Phys.* **2011**, *13*, 886–910.
- Shiraishi, Y.; Saito, N.; Hirai, T. *J. Am. Chem. Soc.* **2005**, *127*, 12820–12822.
- Kim, T. W.; Hur, S. G.; Hwang, S.-J.; Park, H.; Choi, W.; Choy, J.-H. *Adv. Funct. Mater.* **2007**, *17*, 307–314.
- Ide, Y.; Matsuoka, M.; Ogawa, M. *J. Am. Chem. Soc.* **2010**, *132*, 16762–16764.
- Ide, Y.; Nakasato, Y.; Ogawa, M. *J. Am. Chem. Soc.* **2010**, *132*, 3601–3604.
- Maeda, K.; Domen, K. *J. Phys. Chem. Lett.* **2010**, *1*, 2655–2661.
- Kudo, A.; Miseki, T. *Chem. Soc. Rev.* **2009**, *38*, 253–278.
- Osterloh, F. E. *Chem. Mater.* **2008**, *20*, 35–54.
- Shiraishi, Y.; Hirai, T. *J. Photochem. Photobiol. C* **2008**, *9*, 157–170.
- Kominami, H.; Tanaka, A.; Hashimoto, K. *Chem. Commun.* **2010**, *46*, 1287–1289.
- Gunjakar, J. L.; Kim, T. W.; Kim, H. N.; Kim, I. Y.; Hwang, S.-J. *J. Am. Chem. Soc.* **2011**, *133*, 14998–15007.
- Kim, T. W.; Ha, H.-W.; Paek, M.-J.; Hyun, S.-H.; Baek, I.-H.; Choy, J.-H.; Hwang, S.-J. *J. Phys. Chem. C* **2008**, *112*, 14853–14862.
- Tada, H.; Jin, Q.; Nishijima, H.; Yamamoto, H.; Fujishima, M.; Okuoka, S.; Hattori, T.; Sumida, Y.; Kobayashi, H. *Angew. Chem., Int. Ed.* **2011**, *50*, 3501–3505.
- Yu, H.; Irie, H.; Shimodaira, Y.; Hosogi, Y.; Kuroda, Y.; Miyauchi, M.; Hashimoto, K. *J. Phys. Chem. C* **2010**, *114*, 16481–16487.
- Ide, Y.; Hattori, H.; Sadakane, M.; Sano, T. *Green Chem.* **2012**, *14*, 1264–1267.
- Okada, T.; Ide, Y.; Ogawa, M. *Chem.—Asian J.* In press; DOI: 10.1002/asia.201101015.
- Sun, H.; Blatter, F.; Frei, H. *J. Am. Chem. Soc.* **1996**, *118*, 6873–6879.
- Shiraishi, Y.; Teshima, Y.; Hirai, T. *Chem. Commun.* **2005**, 4569–4571.

- (25) Shiraishi, Y.; Ohara, H.; Hirai, T. *J. Catal.* **2008**, *254*, 365–373.
- (26) Shiraishi, Y.; Ohara, H.; Hirai, T. *New J. Chem.* **2010**, *34*, 2841–2846.
- (27) Tsukamoto, D.; Shiro, A.; Shiraishi, Y.; Hirai, T. *J. Phys. Chem. C* **2011**, *115*, 19782–19788.
- (28) Sasaki, T.; Kooli, F.; Iida, M.; Michiue, Y.; Takenouchi, S.; Yajima, Y.; Izumi, F.; Chakoumakos, B. C.; Watanabe, M. *Chem. Mater.* **1998**, *10*, 4123–4128.
- (29) Fuse, Y.; Ide, Y.; Ogawa, M. *Bull. Chem. Soc. Jpn.* **2008**, *81*, 767–772.
- (30) Yanagisawa, T.; Kuroda, K.; Kato, C. *Reactivity Solids* **1988**, *5*, 167–175.
- (31) Ide, Y.; Ogawa, M. *Chem. Commun.* **2003**, 1262–1263.
- (32) Sasaki, T.; Ebina, Y.; Kitami, Y.; Watanabe, M.; Oikawa, T. *J. Phys. Chem. B* **2001**, *105*, 6116–6121.
- (33) Ide, Y.; Ogawa, M. *Angew. Chem., Int. Ed.* **2007**, *46*, 8449–8451.
- (34) Ide, Y.; Nakamura, N.; Hattori, H.; Ogino, R.; Ogawa, M.; Sadakane, M.; Sano, T. *Chem. Commun.* **2011**, *47*, 11531–11533.
- (35) Suzuki, E.; Nakashiro, K.; Ono, Y. *Chem. Lett.* **1988**, 953–956.
- (36) Kim, T. W.; Hwang, S.-J.; Jhung, S. H.; Chang, J.-S.; Park, H.; Choi, W.; Choy, J.-H. *Adv. Mater.* **2008**, *20*, 539–542.
- (37) Ide, Y.; Iwasaki, S.; Ogawa, M. *Langmuir* **2012**, *27*, 2522–2527.
- (38) Sahle-Demessie, E.; Gonzalez, M.; Wang, Z.-M.; Biswas, P. *Ind. Eng. Chem. Res.* **1999**, *38*, 3276–3284.